The 2010 IEEE/RSJ International Conference on
Intelligent Robots and Systems
October 18-22, 2010, Taipei, Taiwan

A NEW CONCEPT OF SELF-RECONFIGURABLE MOBILE MACHINING CENTERS

Hai Yang* , Sébastien Krut†, Cédric Baradat* and François Pierrot†
* Industrial Systems Unit, Fatronik France Tecnalia
34960, Montpellier France
Email: (hyang, cbaradat)@fatronik.com
† Univ. Montpellier 2, CNRS, LIRMM, 161 rue Ada
34392 Montpellier, France
Email: (krut, pierrot)@lirmm.fr

***Abstract*— In this paper, several considerations for designing industry oriented robots which combine the mobility of legged robots and advantages of parallel mechanisms are outlined. A tripod and a quadruped with the same kind of legs are studied. The robots' kinematic models are built for achieving the machining and walking scenarios. The simulations show that: integrating some clamping devices and some lockable passive joints, six actuators are enough to build a legged manipulator which can not only perform 6-axis machining but can also walk on a curved supporting media. Using the "modified condition number" index, the two mechanisms are compared. They have similar workspaces and static wrench performances during the machining phase. During walking processes, however, their behaviors are different, and each of them shows interesting features depending on application requirement.**

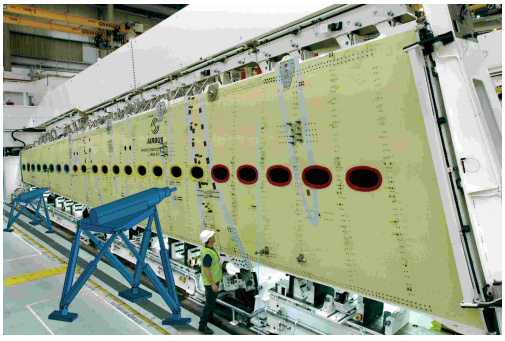

Fig. 1: Artist view of what can be legged drilling robots working on a wing box

I. INTRODUCTION

Legged robots have attracted attention because of their relatively good terrain pass-over capacity [1]. Most of these studies focus on improving the mobility and the reliability of mobile platforms in hazardous environments for exploration purposes. Many legged robot prototypes which imitate the limb structures of animals have been built and studied in universities and research centers.

However, few of them have been used to solve industrial problems: both the human-like biped and animal-like quadruped or hexapod have legs with all their joints being actuated. Three actuators are needed for positioning the pinpoint-type foot to a point in the 3D space where no orientation capacity is required [2]. That is why a typical bio-mimetic quadruped has 12 actuators and a hexapod has 18 actuators. When the orientation of the foot needs to be controlled to fit well the terrain, more than 5 actuators are needed in each leg.

It is difficult to consider using this kind of legged robots for manufacturing applications due to their high material cost and the complexity of their control. Designing a legged robot for manufacturing purpose is very different from designing a legged robot for exploration of hazardous unknown environments [3].

An innovative solution which combines the mobility of legged robot and advantages of parallel mechanism is studied in this paper (Fig. 1 shows an illustration of such robots). In the following sections, several considerations for designing such robots are discussed. Two mobile robots (a tripod and a quadruped) which "walk" on surfaces with moderate curvature and behave like 6-axis parallel manipulators once they are deployed at their working position are presented. A scenario of walking and machining of the tripod is realized based on the derived kinematic models. Jacobian matrices are established by using the screw theory. The workspaces and wrench performances of the two mechanisms are analyzed based on the "modified condition number" index.

II. PRINCIPLES TO REDUCE THE NUMBER OF ACTUATORS

Several techniques are discussed below in order to build industry oriented legged robots which are capable to achieve tasks with high stiffness and accuracy.

a) Sharing Actuators for Positioning each Limb: The body of a legged robot can be moved to help positioning its limbs[1]. Generated by the supporting limbs, the DOFs of the body can be used to position the swinging limb. Instead of actuating each limb independently, sharing actuators for positioning limbs will help to reduce the total number of actuators [4], [5].

[1]The kinematic chains which connect the payload platform and the terrain are hereafter called limbs or branches

(a) Picture of Roptalmu

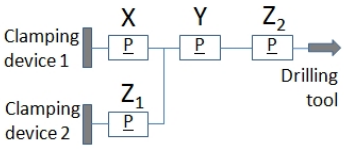

(b) Joint-and-loop graph of the crawler

Fig. 2: Roptalmu, a drilling robot, with multiple functional X-axis

b) Using the Same Actuators for Locomotion and for Manipulation: For conventional mobile robots, the locomotion actuation and the manipulation actuation are usually provided by two independent systems. In order to reduce the number of actuators, the mobility of the locomotion system can also be used for manipulation purpose [6]–[11]. For example, Roptalmu, a 3-axis drilling robot designed for aeronautic industry applications, is composed by a wheeled mobile platform and a crawler robot. The wheeled mobile platform follows automatically the crawler, and its main goal is to compensate the gravity by exerting an upward vertical force on the crawler (Fig. 2 a). As it is outlined in the joint-and-loop graph (Fig. 2 b), actuators X, Z_1 are used for locomotion tasks. And actuators X, Y, Z_2 are used for drilling tasks. Using the X axis actuator for both locomotion and machining tasks makes the mechanism of the crawler more efficient.

c) Integrating Lockers on the Passive Joints: Legged robots, with closed **K**inematic **C**hains (KC) formed between the body and the terrain, can be considered as parallel mechanisms. Noticing that the existence of passive joints in the branches of conventional parallel robots helps to build light-weight robot with relatively higher rigidity, passive joints will be introduced in the design of legged robots for this purpose. However, in order to keep the mechanism controllable during locomotion, lockers should be integrated on some of the passive joints. These lockers can eliminate temporarily the passive DOF when it is necessary [12].

d) Docking System: For robots which are supposed to provide high manipulation stiffness and accuracy, solid connections between the robot and the supporting media (tooling, workpiece itself, etc.) are required. The connection force can be provided by a magnetic device, a vacuum device or a mechanical clamping system [12].

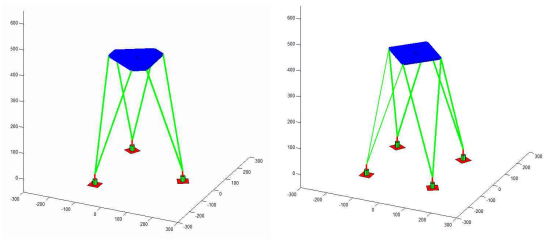

Fig. 3: Matlab sketch of the tripod and quadruped

III. DESCRIPTION OF THE WALKING PARALLEL ROBOTS

Two mobile machining centers (a tripod and a quadruped) with same branch structures are proposed for achieving the required tasks. The proposed mechanism (shown in Fig. 3) can machine as a parallel machining center and walk as a legged robot.

A. Branch's Structure

Branches involved in the two robots have 6-DOF, 2 of them being actuated. From a technical point of view, it is favorable to actuate the prismatic joints for tasks with heavy loads. A structure which has 2 prismatic joints in the KC can be used in the case where 2 actuators are expected. Fig. 4 (a) shows such mechanism in which a 2-DOF planar structure is formed between the three parallel axes (a, b and c). Fig. 4 (b) shows its equivalent serial UPS KC.

B. Geometry of the Platform

With three or four identical branches mounted symmetrically on **P**ayload **P**latform (PP), the tripod and the quadruped shown in Fig. 3 can be obtained respectively. The geometry of the tripod[2] can be described by the geometric parameters (Fig. 5) and the joints variables (Fig. 6).

Branches are symmetrically mounted on the PP, the axes of the last joints of every branch being coplanar. ψ_p, defined as the angles between the axes of the last joints of every

[2]Because of the structure similarity of the two robots, the following geometric description will only concentrate on the tripod. Variable subscripts, which are the indices of the branches, need to be increased to 4 in the case of the quadruped

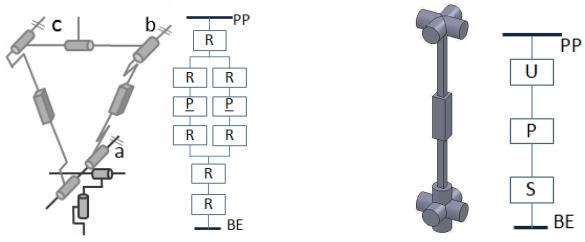

(a) Closed KC (b) UPS KC

Fig. 4: Branch with closed KC and its equivalent UPS KC

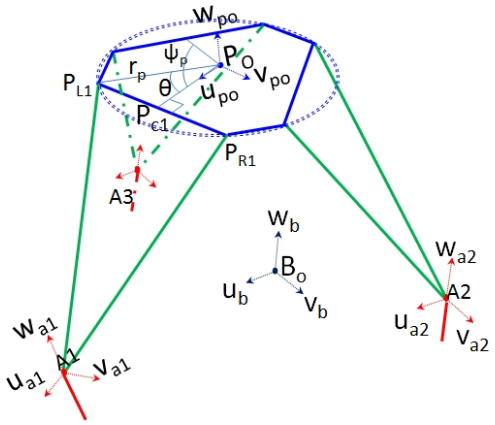

Fig. 5: General coordinates of robot

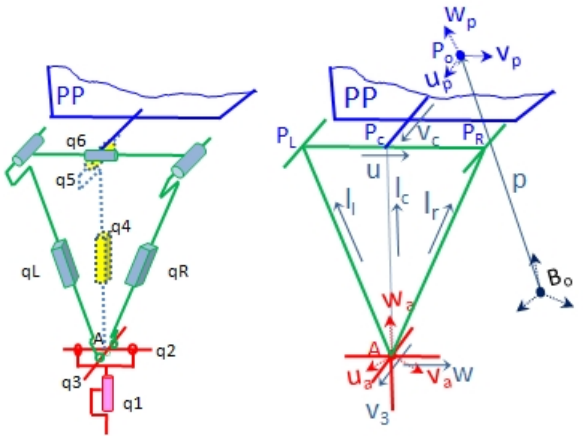

(a) Joints variables (b) Vector model

Fig. 6: Configuration and notations of branches

branches, equals to $\frac{2\pi}{3}$ (tripod) and $\frac{\pi}{2}$ (quadruped). The branch i is connected to the PP at $P_{Li}P_{Ri}$. P_{Ci} is the middle point of $P_{Li}P_{Ri}$, where the virtual serial chain connects to the PP. r_p is the radius of the circle which passes through the connecting points P_{Li}, P_{Ri} of all branches. It defines the size of the PP. θ is the angle between P_OP_{Li} and P_OP_{Ci}. Fixed at the center of the circle P_O, the frame $P_O - u_pv_pw_p$ is attached on the PP with the u-axis pointing to P_{c1}. The frame $B_O - u_bv_bw_b$ is the world frame which is fixed on the supporting media. Limbs frame $A_i - u_{ai}v_{ai}w_{ai}$ $_{(i=1,2or3)}$ is defined for each limb, with its origin located at the point Ai of the ith limb.

The platform pose variable X (x_P; y_P; z_P; α_P; β_P; γ_P) describes the pose (position and orientation) of the frame $P_O - u_pv_pw_p$ regarding to the world frame B_O. $[x_p, y_p, z_p]^T$ is the position vector of the point P_O written in the world frame. α_P, β_P and γ_P are the rotations about the fixed u_b, v_b and w_b axes of the world frame.

The branch extremity variable XAi (x_{Ai}; y_{Ai}; z_{Ai}; α_{Ai}; β_{Ai}; γ_{A_i})$_{(i=1,2or3)}$ describes the pose of frame $A_i - u_{ai}v_{ai}w_{ai}$ regarding to the world frame. $[x_{Ai}, y_{Ai}, z_{Ai}]^T$ is the position vector of point A_i in the world frame. α_{Ai}, β_{Ai} and γ_{Ai} are the rotations about the fixed u_b, v_b and w_b axes of the world frame.

The actuator variable $Q = [qL_{L1}, qR_{L1}, qL_{L2}, qR_{L2}, qL_{L3}, qR_{L3}]^T$. It represents the generalized actuation coordinates vector which corresponds to the displacement of the 6 prismatic joints in the three branches of the robot. The subscripts $L1$, $L2$ and $L3$ are the indices of the three branches.

As it is issued in the previous section, the closed KC configuration, which provides the possibility to use 2 identical linear actuators, can be considered as a virtual UPS serial KC. S_i is the joint values of the virtual serial chain of the i^{th} branch. $S_i = [q_{1Li}, q_{2Li}, q_{3Li}, q_{4Li}, q_{5Li}, q_{6Li}]^T_{(i=1,2or3)}$

IV. WORKING MODES OF THE ROBOTS

The various working modes of the two robots can be roughly distinguished as: **P**ayload **P**latform (PP) control mode and **B**ranch **E**xtremity (BE) control mode. We will see in next section how these two modes are used to perform machining and locomotion.

PP Mode: All branches of the robots are attached to the supporting media. The tripod which are capable of performing 6-axis tasks can be considered as a 6-3 Steward platform from a topological point of view. For the quadruped, there is actuation redundancy.

BE Mode: One branch of the robot is detached from the base in order to reach another supporting point, while the other branches remain attached on the base. For both the tripod and the quadruped, passive joints in the swing branch should be locked in order to control the extremity of this branch before detaching the branch from the supporting point. Furthermore, as there are less branches connected between the PP and the base, the actuators in the branches attached to the base are no longer sufficient to control the PP for the tripod. Some of the passive joints in these branches also need to be locked in order to reduce the DOF of the PP. Such problem does not exist for the quadruped, as while one branch is detached from the supporting point, the 6 DOF of the PP are still fully controllable by actuators located in the 3 left attached branches.

V. MACHINING AND WALKING SCENARIOS SIMULATION OF THE TRIPOD

A. Working Scenario

A working scenario (Fig. 7) which presents one operation cycle from one work location to another can be decomposed into different phases summarized as follows:

Machining phase: With all branches attached to the supporting points, the robot works as a parallel manipulator. By using the **I**nverse **K**inematic **M**odel (IKM), the PP of the manipulator is capable to follow a given trajectory in its workspace. It is important to notice that when the supporting pattern changes, the workspace and force capacity of robot vary as well. This provides the possibility to reconfigure robots for various tasks.

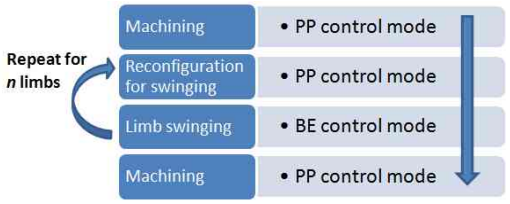

Fig. 7: General scenario

Reconfiguration for limb swinging phase: During this phase, all limbs of the robot are still attached on the supporting points. Before locking the corresponding lockable joints, the PP is supposed to move to a specific position with a given pose in order to have all the B_i joints (defined later in this section) in desired positions for locking.

Limb swinging phase: With the corresponding lockers activated, the extremity of the swinging limb can follow a given 6-axis trajectory.

B. Payload Platform Position Control

The IKM used for the PP position control is the usual model of classical parallel robots which is based on the vectors loop equations [13].

C. Branch Extremity Position Control

When one of the limbs is detached from its supporting point, a hybrid mechanism is formed: a 6-DOF parallel mechanism with 4 actuators plus a 6-DOF mechanism with 2 actuators mounted on the PP.

In BE control mode, in order to control the branch extremity, there should not be passive connectivity between the extremity of the swinging limb and its base. Therefore, the passive joints q_1, q_2, q_3 and q_6 of the swinging limb will be locked before the limb detaches from its supporting point. For the same reason, in order to control the PP with the 4 remaining actuators located in the two supporting limbs, the two q_1 joints (one in each limb) should be locked before the swinging phase begins.

We introduce variable B_i which denotes the locked joints during the swinging phase of limb i : (q_{1Li}; q_{2Li}; q_{3Li}; q_{6Li}; q_{1Lj}; q_{1Lk}) for $((i,j,k) \in \{(1,2,3),(2,1,3),(3,1,2)\}$; i: branch in swing; j, k: branches in stance)

The pose of the branch extremity of the i^{th} limb are described by the BE coordinate variable XAi. So the inverse kinematics problem of the BE mode will be naturally considered as : finding the actuator variable Q with the given value of XAi. Similar to the forward kinematics problems of a conventional parallel manipulator, the direct relationship between XAi and Q are difficult to obtain due to the highly nonlinear equations (polynomial up to 40 degrees in some cases) [14].

To solve this relationship, the problem is formulated in a different way: we consider that the lockers on the lockable joints are not activated, which means the robot works as in PP mode. Then if the pose of a clamping point is changed slightly, the robot will still be capable to keep the platform at the same pose by modifying the values of actuator variable Q. Consequently, the values of the lockable joints B_i will be changed as well. To compute the values of these passive lockable joints, an inverse kinematics model B_iIKMX with X as input and B_i as output is established.

The vector projection approach is used to solve $BiIKMX$. When the relations are valid for every branch independently, the subscripts of variables which indicate the index of branches will be omitted in the equations.

The signed angle between two intersected unit vectors is computed as follows:

$$\Theta(\vec{V}_1,\vec{V}_2,\vec{N}) = \arctan 2(\vec{N}\cdot(\vec{V}_1\times\vec{V}_2),\vec{V}_1\cdot\vec{V}_2) \tag{1}$$

where $\vec{V}_1$,$\vec{V}_2$ are two coplanar unit vectors, $\vec{N}$ is the normal of such plane.

BiIKMX Computation: Let $\vec{v}_c$ be the direction vector of $\overrightarrow{B_OP_C}$, $\vec{u}$ be the direction vector of $\overrightarrow{P_LP_R}$, $\vec{l}_c$ denotes the direction vector of $\overrightarrow{AP_C}$ (Fig. 6 b). q_6 is defined as the angle between plane P_LP_RA and plane $P_OP_LP_R$. As the two planes intersect at P_LP_R, $\vec{v}_c$ is perpendicular to $\vec{u}$, q_6 can be expressed as:

$$q_6 = \frac{\pi}{2} - \Theta({}^{\perp u}\vec{l}_c,\vec{v}_c,\vec{u}) \tag{2}$$

where ${}^{\perp u}\vec{l}_c$, the direction vector of the portion of $\vec{l}_c$ which is perpendicular to $\vec{u}$, is calculated as:

$${}^{\perp u}\vec{l}_c = \frac{\vec{l}_c - (\vec{l}_c\cdot\vec{u})\times\vec{u}}{\|\vec{l}_c - (\vec{l}_c\cdot\vec{u})\times\vec{u}\|} \tag{3}$$

And q_5, being the angle between the P_LP_R and AP_C, can be calculated as:

$$q_5 = \frac{\pi}{2} - \Theta(\vec{u},\vec{l}_c,\vec{u}\times\vec{l}_c) \tag{4}$$

q_4 can be expressed as the distance between P_C and A:

$$q_4 = \|\overrightarrow{B_OP_C} - \overrightarrow{B_OA}\| \tag{5}$$

with $\overrightarrow{B_OP_C} = {}^pR_b \times \overrightarrow{P_OP_C} + \overrightarrow{B_OP_O}$,
where ${}^bR_p$ is the 3×3 rotation matrix from the world frame B_O to the frame P_O: ${}^pR_b = RotZ(\gamma_P)RotY(\beta_P)RotX(\alpha_P)$.

The angle between the projection of Z_a on the plane P_LP_RA and $\vec{l}_c$ equals q_3. $\vec{v}_3$, the direction vector of the q_3 axis, is always perpendicular to the plane P_LP_RA. The direction vector of the projection of Z_a on the plane P_LP_RA can be calculated as ${}^{\perp v3}\vec{v}_{za}$

$${}^{\perp v3}\vec{v}_{za} = \frac{\vec{v}_{za} - (\vec{v}_{za}\cdot\vec{v}_3)\times\vec{v}_3}{\|\vec{v}_{za} - (\vec{v}_{za}\cdot\vec{v}_3)\times\vec{v}_3\|} \tag{6}$$

Therefore, we have

$$q_3 = \Theta(\vec{l}_c,{}^{\perp v3}\vec{v}_{za},\vec{v}_3) \tag{7}$$

The value of joint q_2 is the angle between ${}^{\perp v3}\vec{v}_{za}$ and the w-axis of the frame A.

$$q_2 = \Theta({}^{\perp v3}\vec{v}_{za},\vec{v}_{za},\vec{u}) \tag{8}$$

Let ${}^{\perp v_{za}}\vec{v}_3$ be the projection of $\vec{v}_3$ on the $x-y$ plane of the frame A

$${}^{\perp v_{za}}\vec{v}_3 = \frac{\vec{v}_3 - (\vec{v}_3\cdot\vec{v}_{za})\times\vec{v}_{za}}{\|\vec{v}_3 - (\vec{v}_3\cdot\vec{v}_{za})\times\vec{v}_{za}\|} \tag{9}$$

then q_1 can be expressed as the angle between the u-axis of the frame A and ${}^{\perp v_{za}}\vec{v}_3$

$$q_1 = \Theta(\vec{v}_{xa}, {}^{\perp v_{za}}\vec{v}_3, \vec{v}_{za}) \tag{10}$$

XIKMBi Computation: In reality, the value of locked joints will not be changed during the BE control mode. So the original branch extremity control problem is transformed as follows: when the supporting points change, finding the good values of actuator variable Q which allow all lockable joints to remain to their given values B_i. As we can obtain straightforwardly the actuator variable Q from the platform coordinates X with the IKM of conventional parallel robots, the problem can be further transformed as: finding X, the very pose of PP, which allows values of all activated lockable joints to remain matching the given B_i.

To answer the previous question, a numerical forward kinematics model $XFKMB_i$ is written as an optimization problem: it consists in finding the X which minimizes $\|B_i IKMX(X) - B_i\|$.

D. Scenarios Simulation

The whole cycle of a working scenario is simulated in Matlab. Combining the models, the scenario presented in Fig. 8 shows the feasibility of the concept of a reduced DOF legged robot with integrated lockable joints to achieve machining and self-reconfiguration.

It is worthy to mention that, during all these phases, there is at most one limb detached from the supporting point. Thanks to the clamping devices and lockers, the robots have always solid connection with the supporting media. Unlike most of the tripods that exist in the literature, the limitation of friction between the feet and the ground, the landing impact force [15] and static or dynamic balance [16] issues are not the major concerns as long as the locking components do not fail.

VI. WORKSPACE AND STATIC FORCE ANALYSIS

In this section, the workspaces and the static force performances of the two mechanisms during the machining phase are studied. Notice that the tripod behaves like a 6-3 Steward platform while the quadruped is a redundant actuated mechanism.

A. Jacobian Matrix

The active joint velocity vector, $\dot{Q}$, is a 6×1 vector[3]:

$$\dot{Q} = \begin{bmatrix} \dot{q}_{L1} & \dot{q}_{R1} & \dot{q}_{L2} & \dot{q}_{R2} & \dot{q}_{L3} & \dot{q}_{R3} \end{bmatrix}^T \tag{11}$$

The twist $\hat{\$}_p$ is the general velocity of the PP.

$$\hat{\$}_p = V_p = \begin{bmatrix} \omega_P \\ v_p \end{bmatrix} \tag{12}$$

where ω_p and v_p are the linear and angular velocities of PP, respectively. The kinematic relationship can be expressed as:

$$J_x \hat{\$}_p = J_q \dot{Q} \tag{13}$$

where J_x and J_q are the forward and inverse Jacobian matrices. To determine J_x and J_q, all joints in the branches

[3]Base on the tripod case, the obtained jacobian matrix is also valid for the quadruped by adding the corresponding items of the 4^{th} branch

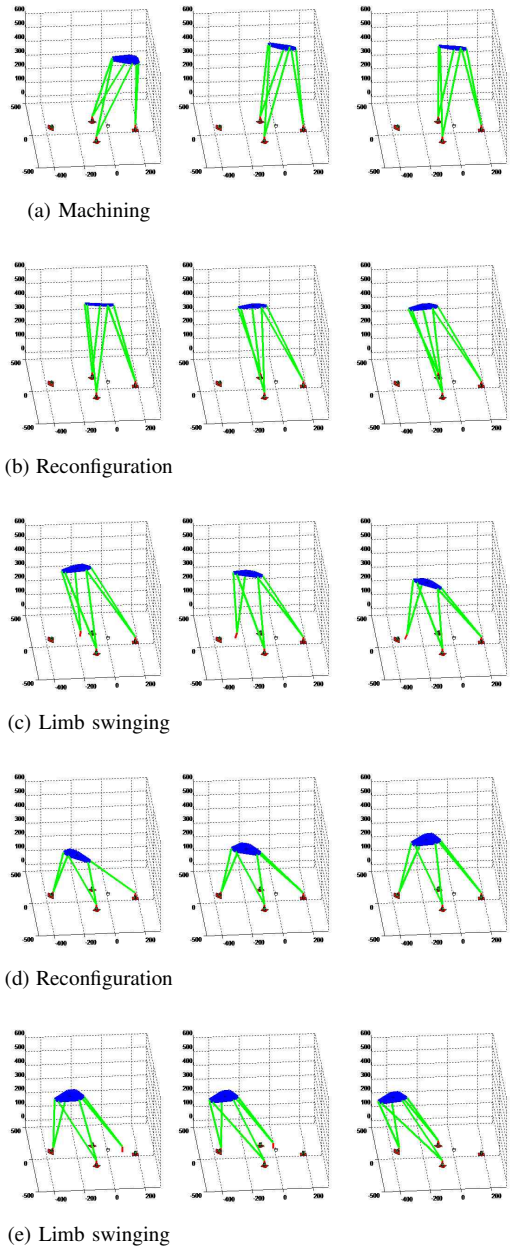

(a) Machining

(b) Reconfiguration

(c) Limb swinging

(d) Reconfiguration

(e) Limb swinging

Fig. 8: Walking and machining scenario

are replaced by twists $\hat{\$}_{iL}$, $\hat{\$}_{iR\ (i=1\cdots6)}$ respectively as denoted in Fig. 9. Considering each branch as an open-loop chain, the instantaneous twist of the PP can be expressed as:

$$\hat{\$}_p = \sum_{i=1}^{6} \dot{q}_{iL} \hat{\$}_{iL} \tag{14}$$

$$\hat{\$}_p = \sum_{i=1}^{6} \dot{q}_{iR} \hat{\$}_{iR} \tag{15}$$

Taking the orthogonal product of both sides of (14) with reciprocal wrench $\hat{\$}_{wL} = \begin{bmatrix} \vec{l}_l \\ \overrightarrow{B_oA} \times \vec{l}_l \end{bmatrix}$ leads to:

$$\hat{\$}_{wL} \circ \hat{\$}_p = \hat{\$}_{wL} \circ \hat{\$}_{4L} \tag{16}$$

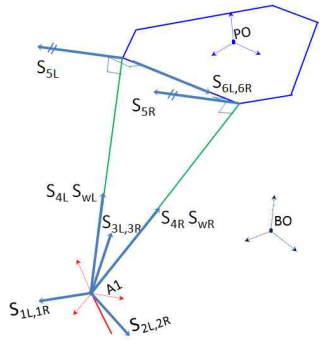

Fig. 9: A branch with its infinitesimal screws

Applying the same operation to (15) with wrench $\hat{\$}_{wR} = \begin{bmatrix} \vec{l}_r \\ \overrightarrow{B_oA} \times \vec{l}_r \end{bmatrix}$ leads to:

$$\hat{\$}_{wR} \circ \hat{\$}_p = \hat{\$}_{wR} \circ \hat{\$}_{4R} \tag{17}$$

Then J_x and J_q in (13) can be determined from (16) and (17):

$$J_x = \begin{bmatrix} (\overrightarrow{B_oA_1} \times \vec{l}_{l1})^T & \vec{l}_{l1}^T \\ (\overrightarrow{B_oA_1} \times \vec{l}_{r1})^T & \vec{l}_{r1}^T \\ (\overrightarrow{B_oA_2} \times \vec{l}_{l2})^T & \vec{l}_{l2}^T \\ (\overrightarrow{B_oA_2} \times \vec{l}_{r2})^T & \vec{l}_{r2}^T \\ (\overrightarrow{B_oA_3} \times \vec{l}_{l3})^T & \vec{l}_{l3}^T \\ (\overrightarrow{B_oA_3} \times \vec{l}_{r3})^T & \vec{l}_{r3}^T \end{bmatrix} \tag{18}$$

and

$$J_q = \begin{bmatrix} 1 & & 0 \\ & \ddots & \\ 0 & & 1 \end{bmatrix}_{(6\times6)} \tag{19}$$

For a spacial mechanism, when the rank of the matrix J_x is less than 6, the PP is no longer fully constrained. In other words, forward singularities occur, when $rank(J_x) < 6$. As the rank of the identity matrix J_q will never reduce, no inverse kinematic singularity exist for the considered mechanism.

B. Static Force Relation

The "inverse" Jacobian matrix J_m represents the linear application linking operational velocities V_p to actuators velocities $\dot{Q}$:

$$\dot{Q} = J_m V_p \tag{20}$$

where $J_m = J_q^{-1} J_x$. Thanks to the conservation of power from actuators to the traveling plate ($\dot{Q}^T f = {V_p}^T w$), the well known relation is obtained.

$$w = {J_m}^T f \tag{21}$$

where w is the wrench of the PP.

As the DOF of PP is a mix between translation and orientation, the weighting matrix W_x for the two proposed robots are defined as

$$W_{x\_tri} = W_{x\_quad} = \begin{bmatrix} \frac{1}{r_p} & 0 & 0 & 0 & 0 & 0 \\ 0 & \frac{1}{r_p} & 0 & 0 & 0 & 0 \\ 0 & 0 & \frac{1}{r_p} & 0 & 0 & 0 \\ 0 & 0 & 0 & 1 & 0 & 0 \\ 0 & 0 & 0 & 0 & 1 & 0 \\ 0 & 0 & 0 & 0 & 0 & 1 \end{bmatrix} \tag{22}$$

where r_p is a chosen characteristic length.

Also, in order to compare the two mechanisms, we assume that actuators of both machines are such that: the sum of maximum forces equals to 1. Then the maximum forces of each actuator is calculated as:

$$f_n = \frac{1}{n} (tripod{:}n{=}6,\ quadruped{:}n{=}8) \tag{23}$$

Then the weighting matrix W_q in terms of actuator performance is defined as:

$$W_q = \begin{bmatrix} f_1 & & 0 \\ & \ddots & \\ 0 & & f_n \end{bmatrix}_{(tripod:n=6),(quadruped:n=8)} \tag{24}$$

Now, introducing (22) and (24) to (21), we have:

$$\widetilde{w} = H\widetilde{f} \tag{25}$$

where $\widetilde{w} = W_x w$, $\widetilde{f} = W_q f$ and $H = W_x {J_m}^T {W_q}^{-1}$
Equation (25) provides the mapping between the admissible actuator force space and the operational wrench space for a given pose.

C. Index of Static Force Analysis

The condition number of H is quite often used as an index to describe the isotropy of a robot. However, in the case where redundant actuation is involved, the condition number is no longer a proper choice for such analysis [17]. In order to study the performance of the tripod and the quadruped, we proposed the following calculations.

The generalized entire acceptable actuator force space is a hypercube defined by the following set:

$$[F] = \{f \mid f_i \in [-f_{max}, f_{max}],\ 1 \le i \le n\} \tag{26}$$

Accordingly, the corresponding set of the generalized resistible wrenches of the PP is:

$$[Z] = \{w \mid \exists f \in [F] \ such\ that\ w = Hf\} \tag{27}$$

Such relation is illustrated in Fig. 10. The notion of w_{MinMax} (the min-max resistable wrench) and w_{Max} (the maximum resistible wrench) are defined in [18]. Notice that these notions are based on the shapes of zonotopes, instead of ellipsoids, in order to describe the exact force capacity and isotropy of a robot [19], [20].

w_{MinMax}, the radius of the largest sphere centered at the origin and that is completely included in the set of resistible wrenches of PP, is defined as

$$w_{MinMax} = \min_{u \in \mathbb{R}^n, \|u\|=1} \left(\max_{\kappa \ge 0} \{\kappa | \kappa u \in z\} \right) \tag{28}$$

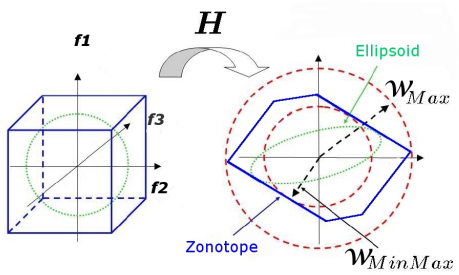

Fig. 10: Illustration of the defined index

w_{Max}, the radius of the smallest sphere centered at the origin and completely contains the set of resistible wrenches of PP, is defined as

$$w_{Max} = \max_{w \in z}(\|w\|) \tag{29}$$

η_w, defined as:

$$\eta_w = w_{Max}/w_{MinMax} \tag{30}$$

reflects the isotropy of the force performance of the mechanism. Notice that this index which can be considered as a kind of modified condition number of H is just one of the proposed method for studying redundant PKM. Recently, Cardou *et al.* [21] proposed novel indices for providing an insight of rotation and translation separately. It can be a meaningful analysis method for our robots when operational tasks are well defined for our robots.

D. Simulated Result

Consider the tripod and the quadruped mechanisms with, $r_p = 100mm$, $\theta = \frac{pi}{4}$ and the branch extremities symmetrically distributed on a circle of radius $r_{pattern} = 180mm$ (as in Fig. 11). The reachabilities of the two mechanisms are tested in a cube ($1000mm \times 1000mm \times 500mm$) located at $500mm$ above the frame B_o orientated along u, v, w axes. Such cube is discretized into M points. $M_{reachable}$ is the number of tested points that do not violate the following conditions:
Condition 1: The length limits of the linear actuators to be:

$$q_{Li,Ri(i=1...4)} \in [390mm, 650mm] \tag{31}$$

where 390 and 650 correspond to the stroke of a classical linear actuator. Condition 2: The largest isotropy wrench at the tested point to be:

$$w_{MinMax} > w_{MinMax\_threshold} \tag{32}$$

Thus, μ_m, the reachability ratio, is defined as:

$$\mu_m = M_{reachable}/M \tag{33}$$

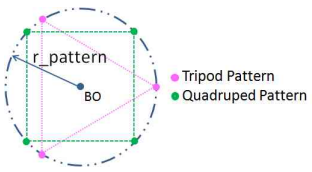

Fig. 11: Supporting pattern of compared mechanisms

TABLE I: PERCENTAGE OF REACHABLE POINTS

$w_{MinMax\_threshold}$	Tripod (μ_m)	Quadruped (μ_m)
0	16.31%	16.04%
0.08	13.60%	14.22%
0.1	9.49%	10.93%
0.12	3.18%	4.58%

TABLE II: AVERAGE INDEX VALUES IN WORKSPACE

Indices	Tripod	Quadruped
w_{MinMax}	0.109	0.113
w_{Max}	1.116	0.857
η_w	10.455	7.746

Table I shows that when KCs are arranged properly, the two mechanisms have similar workspaces. Although the intersection of 3 spheres is supposed to be greater than the one of 4 spheres, the tripod does not have a reachability much greater than the quadruped. When insuring minimum isotropy wrench on the PP by increasing the threshold of w_{MinMax}, the quadruped shows even a better performance in term of reachability.

Table II shows the average values of w_{MinMax}, w_{Max} and η_w calculated numerically in the predefined workspace ($M_{reachable}$ points) with $w_{MinMax\_threshold}$ set arbitrarily to 0.08.

Fig. 12 shows the modified isotropy index (η_w) at three different heights in the predefined workspace.

These results show that: (1) The two mechanisms have similar workspaces; (2) The quadruped has a more homogenous static force performance than its counterpart in the workspace.

VII. DISCUSSION AND PERSPECTIVES

The previous simulation and analysis reveal some important issues for the design of a realistic legged mobile robot with lockable joints.

During the machining phase: (1) The workspace is not really penalized by adding a KC between the PP and the base. The studied mechanisms have very similar behavior during the machining phase. (2) From the topological point of view, each robot keeps the same kinematics in each working area. However, when the supporting pattern (configurations of the supporting points (A_i)) changes, the robot has no longer the same geometrical parameters. The workspace, the rigidity, the isotropy and many other properties of the robot vary as well.

During the walking phase: (1) The fact that the tripod has only two contacts with the supporting media requires large locking force to support the robot's weight. Unlike the tripod, light duty lockers can be used for the quadruped. (2) The extremity of the swinging limb of the tripod is controlled by 6 actuators. For a given pose of the extremity of the swing limb, the tripod has no kinematics redundancy, so cannot control the PP to avoid interferences with environment. Meanwhile, the significant advantages of the quadruped is

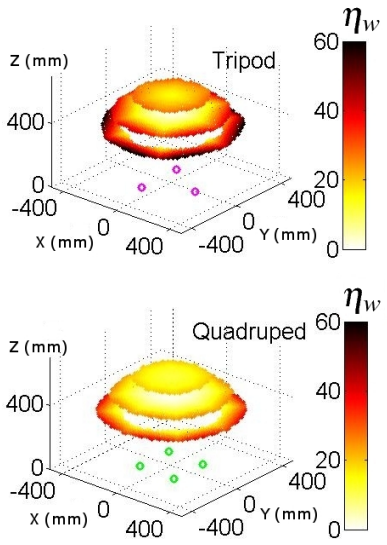

Fig. 12: η_w at different height in the workspace

that, during the walking phase, the connectivity between BE link and the supporting surface is eight, which provides the possibility to follow its own given trajectory and to optimize the PP trajectory at the same time. This might be an important issue for applications which have strong geometrical constraints in the environment.

Strategy for locking joints: The choice of lockable joints configuration has a significant impact on the size of the reachable walking area of the robot. This will be studied in future work.

VIII. CONCLUSION

In this paper, several considerations for designing industry oriented legged robots were highlighted. Two proposed mobile manipulators which overcome the drawbacks of both parallel robots and legged mobile robots were studied. With the derived kinematic models, a scenario of machining and walking of the tripod is simulated in order to demonstrate the principles of this kind of mobile machining centers. We show that: integrating lockers on some passive joints and some clamping media, 6 actuators are enough to build a legged manipulator which can not only achieve 6-axis machining but also walk on a curved continuous and/or discontinuous supporting media. Furthermore, using the "modified condition number", the studies of resistible external static wrench show that the two mechanisms have similar workspaces and static force performances during the machining phase. During the limbs' swinging phase, kinematic redundancy of the quadruped makes it a reasonable choice for the applications with strict geometrical constraints in the environment. Further studies on kinematics, dynamics, as well as the supporting points arrangement, will be done in order to design such robots with optimized performance for machining and walking.

REFERENCES

[1] J. E. Pablo Gonzalez de Santos, Elena Gracia, *Walking robots*. Springer London, 2007, ch. Quadrupedal Locomotion, pp. 3–32.

[2] K. Yoneda and Y. Ota, "Non-bio-mimetic walkers," *The International Journal of Robotics Research*, vol. Vol. 22, No. 34,, pp. 241–249, 2003.

[3] K. Inagaki, *Reduced DOF Type Walking Robot Based on Closed Link Mechanism*. I-Tech, Vienna, Austria, 2007, ch. Bioinspiration and Robotics: Walking and Climbing Robots, Book, p. 554.

[4] G. R. Dunlop, "Foot design for a large walking delta robot," in *Experimental Robotics VIII*. Springer Berlin / Heidelberg, 2003, pp. 602–611.

[5] J. M.Sabater, R. J. Saltaren, R. Aracil, E. Yime, and J. M. Azorin, "Teleoperated parallel climbing robots in nuclear installations," *Industrial Robot: An International Journal*, vol. 33, pp. 381–386, 2006.

[6] T. Arai, N. Koyachi, H. Adachi, and K. Homma, "Integrated arm and leg mechanism and its kinematic analysis," in *Robotics and Automation, 1995. Proceedings., 1995 IEEE International Conference on*, vol. 1, Nagoya, Japan, May 1995, pp. 994–999.

[7] Y. Takahashi, T. Arai, Y. Mae, K. Inoue, and N. Koyachi, "Development of multi-limb robot with omnidirectional manipulabilityand mobility," in *Intelligent Robots and Systems, 2000. (IROS 2000). Proceedings. 2000 IEEE/RSJ International Conference on*, vol. 3, Takamatsu, Japan, 2000, pp. 2012–2017.

[8] V. Collado, J. Arana, and A. Saenz, "A crawling portable robot for drilling operations in large air frame components," *SAE International*, vol. 1, p. 3337, 2005.

[9] N. Koyachi, H. Adachi, M. Izumi, T. Hirose, N. Senjo, R. Murata, and T. Arai, "Control of walk and manipulation by a hexapod with integrated limb mechanism: MELMANTIS-1," in *Robotics and Automation, 2002. Proceedings. ICRA '02. IEEE International Conference on*, vol. 4, 2002, pp. 3553–3558.

[10] R. M. Voyles and A. C. Larson, "Terminatorbot: a novel robot with dual-use mechanism for locomotion and manipulation," *IEEE/ASME Transactions on Mechatronics*, vol. 10, no. 1, pp. 17–25, Feb. 2005.

[11] V. Collado, A. Saenz, J. Gonzalez, and J. R. Astorga, "Roptalmu - a new concept of crawling portable robotic system for wing spars drilling," *SAE International*, vol. 09ATC, p. 0037, 2009.

[12] F. Aghili, "A conceptual design for reconfigurable robots," Canadian Space Agency, Tech. Rep., 2004.

[13] D. Stewart, "A platform with six degrees of freedom," *Aircraft Engineering and Aerospace Technology*, vol. Volume:38 Issue:4, pp. 30–35, 1966.

[14] J. Nielsen and B. Roth, "On the kinematic analysis of robotic mechanisms," *The International Journal of Robotics Research*, vol. Vol. 18, No. 12, pp. 1147–1160, 1999.

[15] K. Hashimoto, A. Hayashi, T. Sawato, Y. Yoshimura, T. Asano, K. Hattori, K. Hashimoto, A. Hayashi, T. Sawato, Y. Yoshimura, T. Asano, K. Hattori, H. ok Lim, and A. Takanishi, "Terrain-adaptive control to reduce landing impact force for human-carrying biped robot," in *IEEE/ASME International Conference on Advanced Intelligent Mechatronics*, 2009.

[16] H. D. Ping Ren, "Triple stance phase displacement analysis with redundant and nonredundant sensing in a novel three-legged mobile robot using parallel kinematics," *Journal of mechanisms and robotics*, vol. Vol.1, Nb.4, 2009.

[17] S. Krut, O. Company, and F. Pierrot, "Velocity performance indices for parallel mechanisms with actuation redundancy," *Robotica*, vol. 22:2, pp. 129–139, 2004.

[18] ——, "Force performance indexes for parallel mechanisms with actuation redundancy, especially for parallel wire-driven manipulators," in *Intelligent Robots and Systems, 2004. (IROS 2004). Proceedings. 2004 IEEE/RSJ International Conference on*, vol. 4, Sep./Oct. 2004, pp. 3936–3941.

[19] P. Chiacchio, "A new dynamic manipulability ellipsoid for redundant manipulators," *Robotica*, vol. 18, pp. 381–387, 2000.

[20] B. Samuel, C. M.Gosselin, and B. Moore, "On the ability of a cable-driven robot to generate a prescribed set of wrenches," in *Proceedings of the ASME Mechanisms and Robotics Conference*, 2008.

[21] P. Cardou, S. Bouchard, and C. Gosselin, "Kinematic-sensitivity indices for dimensionally nonhomogeneous jacobian matrices," *IEEE TRANSACTIONS ON ROBOTICS*, vol. Vol.26 No.1, pp. 116–173, 2010.